Dynamic Analysis of a Transient Plucking Energy Harvester towards Battery-free Motion-Sensing System

Xin Li, Guobiao Hu, Hong Tang, Yue Zhu, Junrui Liang*

School of Information Science and Technology, ShanghaiTech University

* Corresponding email: liangjr@shanghaitech.edu.cn

Abstract:

This paper introduces a transient plucking energy harvester towards a battery-free motion-sensing IoT system. A piezo-magneto-elastic system composed of a low-cost piezoelectric cantilever and a pair of magnets is used to form a plucking mechanism for high-efficient energy harvesting in response to a transient external excitation. Instead of investigating the frequency-up conversion and expecting a continuous power supply from the harvester, we give a comprehensive analysis to explore how much energy the harvester can capture from the single plucking motion. The energy flow transformations with the potential energy pre-charging, the varying potential energy pictures during the plucking process, and the dynamic behaviors under the influence of different magnet layouts are numerically investigated. Moreover, we implemented a prototype ViPSN-pluck based on a co-design considering the cyber-electromechanical synergy. Only one plucking can fulfill the tasks of motion direction detection and wireless transmissions. The proposed ViPSN-pluck provides valuable guidance towards the design of kinetic energy harvesting IoT systems.

Keywords: vibration energy harvesting; plucking; bistable; transient; battery-free IoT

1. Introduction

Energy harvesting has emerged as a promising power solution for Internet of Things (IoT) systems via leveraging ambient energy sources such as solar, radio frequency (RF), and vibration. Free from chemical batteries, these energy harvesting-powered IoT systems are not only self-sustaining and maintenance-free, but also eco-friendly [1]. They have been deployed in many application domains, such as infrastructure monitoring, in-body medical sensing, and space exploration. In particular, kinetic energy in the form of vibrations, random displacements, or forces is ubiquitous

and versatile in our ambient environment [2]. It covers direct human activities from walking, running, finger tapping, heartbeat, to respiration; structural vibrations from industrial machinery, buildings, and transport vehicles; fluid flows from wind, water, ocean, etc. Kinetic energy harvesting (KEH) has caught great attention from various disciplines. It has been widely recognized as one of the most viable solutions to address the sustainable power supply issue for realizing battery-free IoT sensors.

In the past two decades, research on KEH has focused on developing strategies to maximize uninterrupted power supply capacity. Namely, within given continuous excitation, broadening the operation bandwidth and improving the electromechanical conversion efficiency, thus providing a reliable and stable power supply *"appear"* like a battery. For example, by introducing nonlinearities [3] or using self-adaptive structures [4], the harvester can adapt to various kinetic sources with different spatial directions, operation patterns, and excitation frequencies. By implementing the synchronized switch harvesting on inductor (SSHI) interface circuits, their power capacity can be increased by about 300–400%, compared to the standard energy harvesting (SEH) case [5].

However, in real-world situations, most ambient kinetic sources are inherently fluctuating, often intermittent, or even transient. Even if some energy harvesters can provide high peak power, the power outputs are unpredictable, and the power outages are inevitable. Furthermore, the sensing, computing, and communication tasks performed by a KEH-powered IoT system have to cope with such limitations and fluctuations [6]. Fundamentally different from the conventional battery-powered counterpart, it violates one of the basic computing assumptions—a stable power supply [7]. Therefore, without considering the ineluctable fluctuations of ambient sources and the unprecedented challenges of computational revolutions for battery-free systems, the separate discussion on the maximum uninterrupted power supply capacity could be misleading [8].

Given the energy constraints under various source conditions, the energy harvesting-based embedded computing system should be designed differently from conventional systems [1]. Hardware and software synergy is necessary for guaranteeing reliable and robust operations in the long run. A device's run-time behaviors, such as when to execute tasks, how to use low-power modes, or when to communicate, determine not only how much energy it consumes, but also how much energy it harvests [9]. For example, opening a drawer can provide 10-30 μJ energy [10], which can support at least

one round of temperature sensing; shaking an object can produce 500-2000 μJ energy [10], which can be used to do several rounds of wireless transmission.

In this paper, we present a transient plucking energy harvester towards a battery-free motion-sensing IoT system. It is composed of a low-cost piezoelectric cantilever and a pair of magnets, which realize a plucking mechanism for high-efficient energy harvesting in response to a transient external excitation. Different from the previous studies, the plucking mechanisms [11] [12] [13] were investigated for the frequency-up conversion, and expecting a continuous power supply from the harvester, we give a comprehensive model and analysis to explore how much energy the harvester can capture from the single plucking motion. Moreover, based on the cyber-electromechanical synergy among mechanical dynamics, power conditioning circuit, and the low-power embedded system, we implement a battery-free motion-sensing system, which is named ViPSN-pluck, as shown in Fig. 1. Via a mechanical modulation, i.e., potential energy pre-charging, ViPSN-pluck can be guaranteed to harvest sufficient energy from a transient motion to execute the subsequent tasks, including motion pattern identification and wireless communication. It also can robustly achieve the plucking motion direction identification based on the principle that the amount of energy harvested from one stroke is correlated with the motion pattern to be detected.

2. Design and Modeling

The design of the transient plucking energy harvester is shown in Fig. 1 and Fig. 2. Based on the magnetic plucking mechanism, two repelling magnets are installed at the piezoelectric cantilevered beam's free end (M1) and the moving host (M2), respectively, for generating the magnetic plucking excitation under a one-way transient movement. In each plucking motion, the cantilevered beam with tip magnet (M1) is bent by a driving magnet (M2) through magnetic force coupling. The cantilevered beam is rapidly released after the magnet pass through a critical position, where the magnetic force could not balance the restoring force of the bent beam. After being released, the cantilevered beam starts to oscillate until the vibration is damped out.

Meanwhile, in the whole plucking process, when the driving magnet moves, the profile of mechanical potential energy (sum of the beam elastic and magnetic portions) progressively changes, which results in the varying potential energy pictures. Each

plucking motion can drive the single-well monostable system to a bistable system, then pass through the potential barrier, i.e., the critical position, and finally reach another monostable system. Moreover, it is easy for the plucking harvester to obtain a distinguishable vibration response by setting the start and stop positions of the driving magnet, as shown in Fig. 2 (a)-(e) and Fig. 3 (a)-(e).

For the magnetic plucking harvester, the total mechanical potential energy (U) is the sum of the elastic energy (U_e) of the cantilevered beam and the magnetic potential energy (U_m) generated by the driving magnet (M2) and the tip magnet (M1).

$$U(w,b) = U_e(w) + U_m(w,b)$$

where w is the cantilevered beam deflection, i.e., the horizontal distance between the beam fixed end and the center of tip magnet (M1); b is the position of the driving magnet (M2).

The elastic potential of the cantilevered beam under bending motion can be given by

$$U_e(w) = \frac{1}{2}Kw^2$$

where K is the bending stiffness. The plucking of the driving magnet results in varying magnetic potential energy, which can be described by the dipole-dipole model.

$$U_m(w,b) = -\frac{\mu_0}{4\pi}(\nabla\frac{\mathbf{m}_{O_2}\cdot\mathbf{r}_{O_1O_2}}{\left\|\mathbf{r}_{O_2O_1}\right\|_2^3})\mathbf{m}_{O_1}$$

where μ_0 is the vacuum permeability; $\mathbf{r}_{O_1O_2}$ denotes the vector pointed from the center of driving magnet (M2) to the center of tip magnet (M1); $\mathbf{m}_{O_1}$ and $\mathbf{m}_{O_2}$ represent the magnetic moment vectors of tip magnet (M1) and driving magnet (M2). For permanent magnets, these magnetic moment vectors can be evaluated as

$$\mathbf{m}_{O_1} = \begin{pmatrix}\frac{B_r V_{O_1}}{\mu_0}\\ 0\end{pmatrix};\ \mathbf{m}_{O_2} = \begin{pmatrix}\frac{B_r V_{O_2}}{\mu_0}\\ 0\end{pmatrix}$$

where B_r is the magnets residual flux density; $\frac{B_r}{\mu_0}$ represents the magnitude of magnetization vector; V_{O_1} and V_{O_2} are the volumes of tip magnet (M1) and driving magnet (M2), respectively.

Hence the varying magnetic potential energy and the plucking magnetic force F_m can be calculated as

$$U_m(w,b) = -\frac{\mu_0 m_{O_1} m_{O_2}}{4\pi}\left(r_{O_2O_1}^{-3} - 3d^2 r_{O_2O_1}^{-5}\right)$$

$$F_m(w,b) = \frac{3\mu_0 m_{O_1} m_{O_2}(w-b)}{4\pi r_{O_2O_1}^5 L}\left\{\frac{dw}{w-b} - \sqrt{L^2-w^2} - \frac{5d}{r_{O_2O_1}^2}\left[w(w-b) - d\sqrt{L^2-w^2}\right]\right\}$$

where m_{O_1} and m_{O_2} are the norms of $\mathbf{m}_{O_1}$ and $\mathbf{m}_{O_2}$; $r_{O_2O_1}$ is the norms of $\mathbf{r}_{O_2O_1}$, i.e., dynamic interval from the center of driving magnet (M2) to that of tip magnet (M1); and d is the dynamic vertical magnet interval. Because the rotation angle α of the tip magnet is small enough to be approximated as that of the cantilevered beam β, the dynamic vertical magnet interval d and the dynamic interval of the magnets $r_{O_2O_1}$ during the plucking process can be expressed as

$$d = d_0 + L - \sqrt{L^2 - w^2}$$

$$r_{O_2O_1} = \sqrt{(w-b)^2 + d^2}$$

where L is the length of the piezoelectric cantilevered beam; d_0 is the initial magnet interval along the vertical direction.

Based on the single-degree-of-freedom (SDOF), the governing equations of the electromechanical model for the transient plucking energy harvester can be obtained as

$$\begin{cases} M\ddot{w} + D\dot{w} + Kw + \Psi_e v_p = \dfrac{dU_m(w,b)}{w} \\ \dfrac{v_p}{R} = \Psi_e \dot{w} - C_p \dot{v_p} \end{cases}$$

where M is the equivalent masses of the piezoelectric cantilevered beam with the tip magnet (M1); D is the damping coefficient; Ψ_e is the electromechanical coefficient; v_p represents the output voltage, and $\frac{v_p}{R}$ is the current flowing through the road R; C_p is the piezoelectric clamped capacitance.

3. Analysis

In order to explore how much energy the harvester can capture during the transient motion excitation, we divide the single plucking action into two phases before and after the critical position, i.e., mechanical potential energy pre-charging and decaying under-damped free vibration. Correspondingly, the energy flow transformations with the potential energy pre-charging, the varying potential energy pictures during the plucking

process, and the dynamic system responses under the influence of overlap length and plucking velocity are numerically investigated. The parameters of the piezoelectric cantilevered beam and repelling magnet are listed in Table 1.

3.1 Potential Energy Pre-charging

Fig. 4 shows the energy flow dynamics under a single plucking excitation. There are four forms of energy involved in this process: mechanical potential energy, mechanical kinetic energy, thermal energy, and electrical potential energy. The energy transformations during this process can be summarized as follows.

1) Plucking start: At the beginning, the energy harvester is at its equilibrium position. We set this position the zero-energy position.

2) Energy accumulation: As the driving magnet forces the cantilevered beam to deform, it does positive work to the cantilevered beam. Assuming a very slow plucking motion, in which the kinetic energy can be neglected, the input energy is collected by the deformed cantilevered beam in the form of strain energy, i.e., the mechanical potential energy of a deformed structure. The potential energy reaches its maximum when the cantilevered beam arrives at the critical position. The total mechanical potential energy at M1 position w and M2 position b can be expressed as follows

$$E_{pre} = U[w_c = w(t_c), b_c = b(t_c)]$$

where w_c and b_c are the positions of tip magnet (M1) and driving magnet (M2) at the critical state, respectively.

3) Under-damped Vibration: After the critical point, the elastic restoring force prevails; the beam is released and begins to oscillate at its resonant frequency, as shown in Fig. 4. During the free vibration of the cantilevered beam, the pre-charged potential energy (E_{pre}) is converted into mechanical kinetic energy, thermal energy, and electrical energy during the under-damped vibration and energy harvesting process. Hence, the pre-charged potential energy (E_{pre}) actually directly determines the total energy that can be harvested.

Only when the converted electrical energy ($E_e = \eta E_{pre}$) exceeds the energy kicking-off threshold, which is denoted as E_{load}, the sensing and wireless communication functions can be fulfilled successfully. The parameter η denotes the electromechanical energy conversion efficiency, which is related to mechanical structure, interface circuit, energy management circuit, and load. In this study, we are neglecting the unpredictable kinetic energy that is sensitive to the pulling speed, ηE_{pre} is regarded as the normal harvestable electrical energy, as shown in Fig. 4. Moreover, the pre-charged potential energy (E_{pre}) can be pre-designed by adjusting the mechanical structure, including the beam geometry and the horizontal distance gap between the driving and tip magnets.

3.2 Potential Energy Pictures

Fig. 2 and 3 show the time-varying potential well pictures for the open-door and close-door processes, respectively. As the driving magnet moves, the potential energy profile progressively changes. As shown in Fig. 2 (a), in the open-door case, at the most beginning, the cantilevered beam is at the static state. Due to the presence of the driving magnet (M2), which has not started to move, the cantilevered beam is slightly bent towards the left-hand side. From the potential well profile of the current state (Fig. 2 (f)), one knows that the cantilevered beam is at a monostable state since there is only a single potential well-1, which indicates a single equilibrium position for the cantilevered beam.

When the driving magnet moves to the left, the cantilever is further bent, and a second potential well-2 may form in the potential profile, indicating the transition from a monostable state to a bistable state. In this process, the potential profile is first asymmetric (Fig. 2 (g)), then becomes symmetric (Fig. 2 (h)), then asymmetric (Fig. 2 (i)) again. Finally, when the driving magnet moves far away from the transient plucking energy harvester, the driving magnet would have a negligible effect on the tip magnet of the cantilevered beam. The potential profile of the cantilevered beam would become linearly symmetric (Fig. 2 (j)), implying that the cantilevered beam would undergo linear vibration.

For the close-door case, the potential profile evolution is illustrated in Fig. 3. As compared with Fig. 2, it can be found that the evolution process of the close-door case is reversed. It starts from a linear state and ends in a nonlinear monostable state. Hence, it is easy to design a transient plucking energy harvester with distinguishable vibration

responses for different plucking directions by calibrating the proper initial position of the driving magnet.

3.3 Dynamic Analysis

Fig. 5 shows the dynamic behaviors with different terminal positions (b_t) of the driving magnet. Correspondingly, as shown in Fig. 2 (j) and Fig. 3 (j) by calibrating the terminal position b_t in one direction and quasi-infinity in the other direction, an asymmetrical design is obtained, i.e., the dynamic behaviors for the two different plucking directions are non-reciprocal. The former case yields a nonlinear monostable vibrator. Fig. 5 (a) and (b) show its dynamic behaviors with beam displacement, displacement-velocity phase trajectory. The latter case corresponds to a linear vibrator. Its dynamic behaviors are shown in Fig. 5 (c) and (d).

Moreover, Fig. 5 (e) and (f) show the dynamic behaviors when the terminal position of the driving magnet is set to 0, i.e., the bistable state, as shown in Fig. 3 (h). As mentioned in the previous section, the cantilevered beam can only be restricted to oscillating in a single well by potential barrier obstruction. Fig. 5 (g) and (h) are the dynamic behaviors when the terminal position of the driving magnet is less than the critical position, i.e., $b_t < b_c$. As shown in Fig. 5(g), with the excitation of external kinetic energy, the cantilevered beam is able to span the potential barrier and oscillates from well #2 to well #1. However, once the external kinetic energy is insufficient, the cantilevered beam can only oscillate in a single well, as shown in Fig. 5 (h). Therefore, according to this feature, the plucking direction can be identified based on how much energy is captured during a single plucking excitation. The energy harvesting performance can be further optimized by further tuning the mechanical structure parameters, such as depth of potential well and height of the potential barrier.

4. Experiment

4.1 System Implementation

In this study, we implement a prototyped ViPSN-pluck, whose picture is shown in Fig. 1. The holding frame of the transient-motion harvester is manufactured using a 3-D printer. The other three units are developed based on ViPSN [14], which is an open-

source development platform specified for vibration-powered IoT devices (https://github.com/METAL-ShanghaiTech/ViPSN).

4.2 Energy Reliability

Fig. 6 shows the energy harvesting performance of the transient plucking harvester under the open-door and close-door excitations. The peak acceleration magnitudes that range from 0.03 g to 0.6 g are measured in real scenarios. Experimental results demonstrate that during each single open/close-door process, ViPSN-pluck can robustly harvest at least 1000 μJ of electrical energy. Only about 201.54 μJ energy is needed to execute one round of BLE IoT module initialization and beacon transmission. Therefore, the harvested energy from a single open/close-door process can definitely support the ViPSN-pluck to complete the desired tasks.

4.3 Plucking Direction Identification

Fig. 7 shows the time responses of the harvester from various aspects during both the open-door and close-door processes. In the open-door process, the transient plucking harvester is first pulled away from its initial equilibrium position, then released to vibrate freely. When the driving magnet moves far away, the free vibration motion of the transient-motion harvester is finally trapped by a single linear well-2, as shown in Fig. 7 (a) and (b). In the close-door process, as the driving magnet gradually approaches, the transient plucking harvester finally undergoes nonlinear vibration in an asymmetric well-1, as shown in Fig. 7 (d) and (e). The experimental results are shown in Fig. 7 (c) and (f) reveal that during the open-door and close-door processes, the transient-motion harvester can produce about 1600 μJ and 1300 μJ of electrical energy, respectively.

The software on the cyber system is optimized to ensure a rapid and robust response. Each activation consists of one initialization and several radio transmissions. It is worth noting that the energy consumption of the beacon broadcasting operation is fixed, about 60.37 μJ. Therefore, according to the motion detection working principle, as explained in the previous section, by counting the number of BLE beacon packets transmitted using the data aggregator, the plucking direction can be identified.

6. Conclusion

This paper introduces a transient plucking energy harvester towards a battery-free motion-sensing IoT system. A magnetic plucking energy harvester is used to scavenge the energy associated with a transient motion. Instead of investigating the frequency-up conversion and expecting a continuous power supply from the harvester, we give a comprehensive analysis to explore how much energy the harvester can capture from the single plucking motion. With the analytical model validated by numerical simulation, we analyze the energy flow transformations with the potential energy pre-charging, the varying potential energy pictures during the plucking process, and the dynamic behaviors under the influence of different magnet layouts.

Moreover, a prototype ViPSN-pluck is implemented and deployed in real-world scenarios. Experimental results show that the energy harvested from a single plucking motion can be up to 1000 μJ, which is sufficient to carry out several rounds of sensing function and wireless transmission. Through the collaboration between the plucking piezoelectric cantilever and the embedded computing system, the movement information, including motion plucking direction, can be identified and sent out with a commercial BLE module. This study provided valuable guidance for the design and optimization of future kinetic energy harvesting IoT systems.

Figure Captions

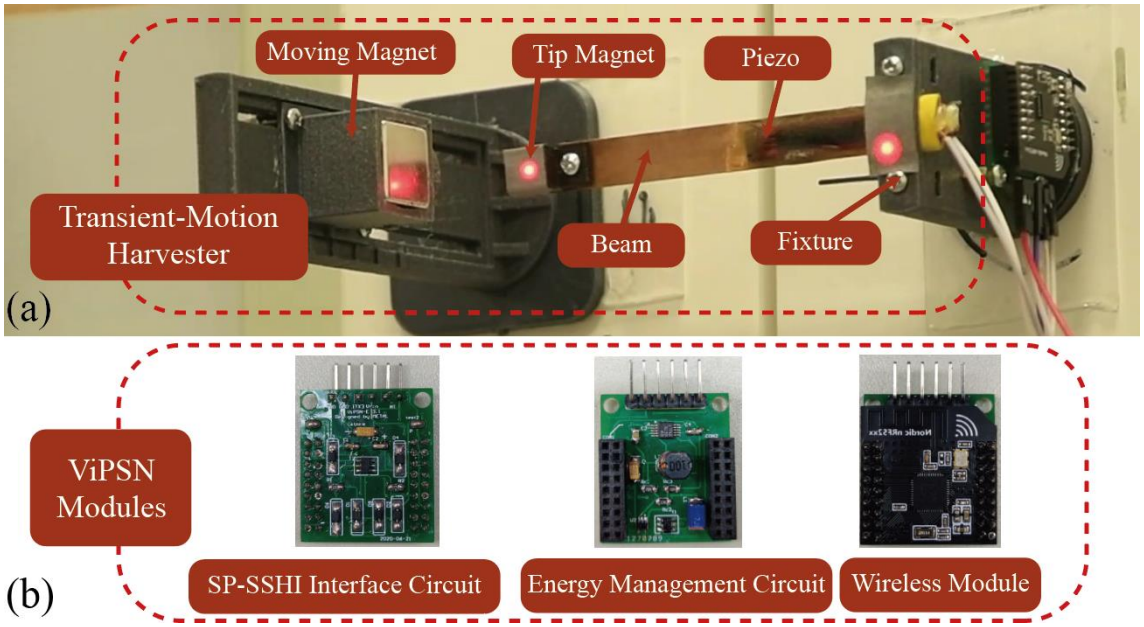

Fig. 1. The prototyped ViPSN-E device. (a) The transient plucking energy harvester. (b) ViPSN modules.

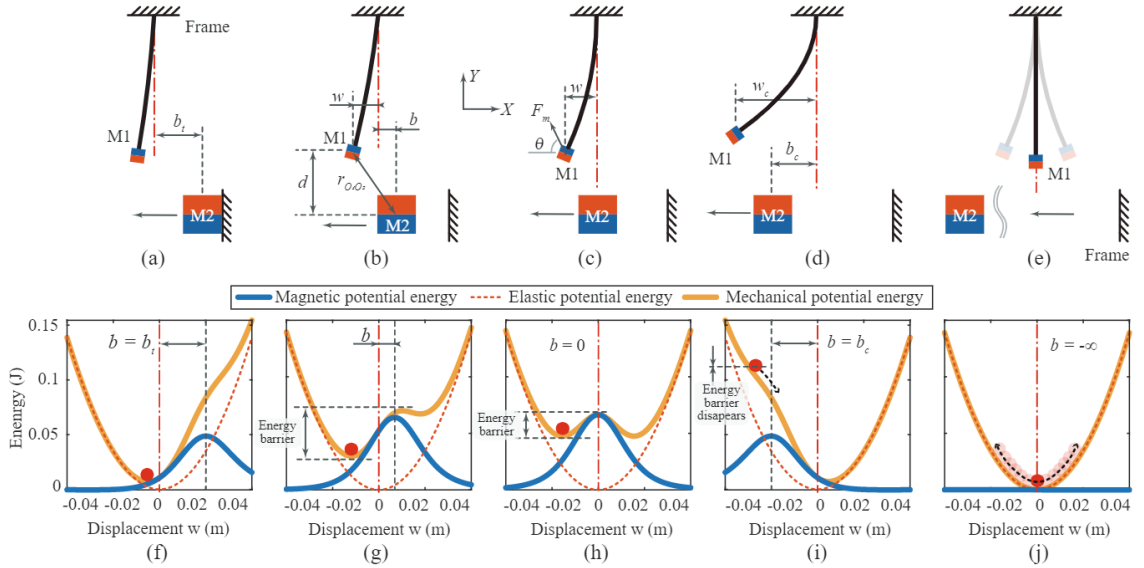

Fig. 2. Plucking dynamics under the plucking movement. (a)-(e) Beam positions. (f)-(j) The corresponding potential wells. (a) and (f) Starting position with a monostable potential well. (b) and (g) Intermediate position with two asymmetric wells. (c) and (h) Intermediate position with two symmetric wells. (d) and (i) Critical position at which the energy barrier disappears. (e) and (j) Final position ending up with the beam vibration in a single linear well.

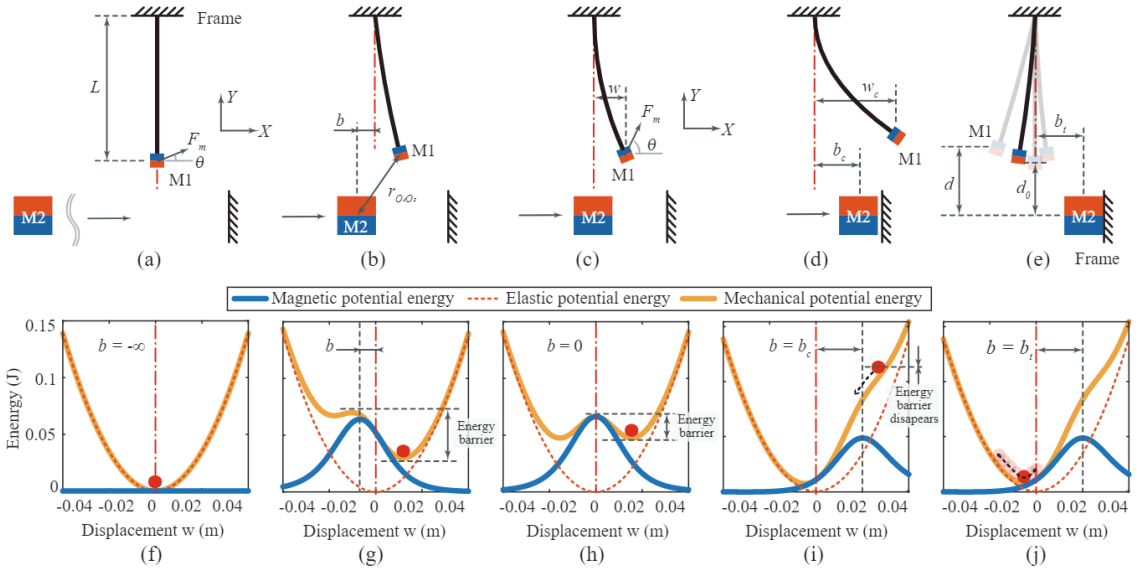

Fig. 3. Plucking dynamics under the plucking movement. (a)-(e) Beam positions. (f)-(j) The corresponding potential wells. (a) and (f) Starting point with a (linear) single well. (b) and (g) Intermediate point with two asymmetric wells. (c) and (h) Intermediate point with symmetric wells. (d) and (i) Critical point at which the energy barrier disappears. (e) and (j) Final point ending up with the beam vibration in a (nonlinear) monostable well.

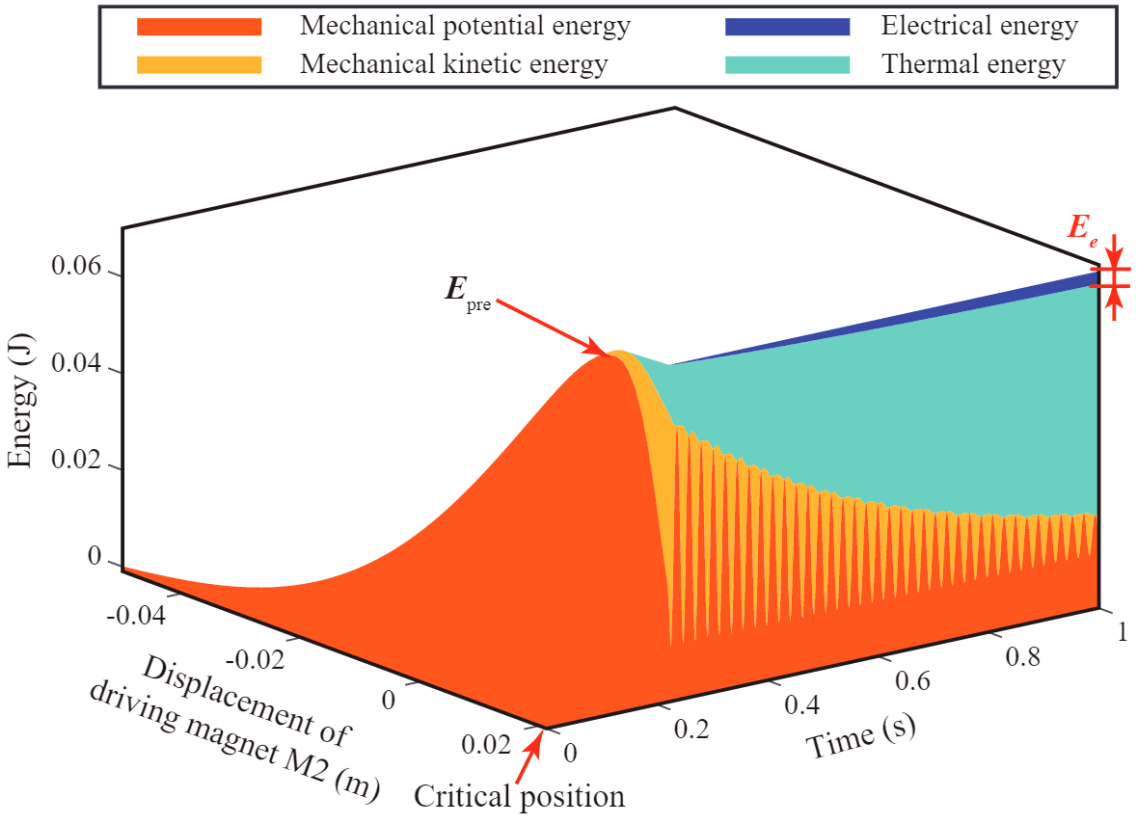

Fig. 4. Energy flow dynamics of the transient plucking energy harvester under a plucking excitation.

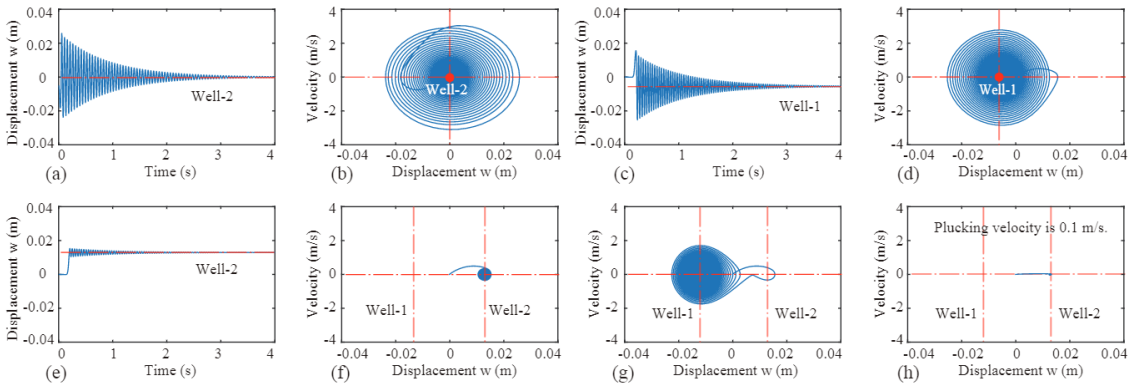

Fig. 5. Dynamic behaviors with different terminal positions (b_t) of the driving magnet. (a) and (b) Linear vibrator, the terminal position is set to infinity, $b_t = -\infty$. (c) and (d) Monostable vibrator, the terminal position is set as the critical position, $b_t = b_c$. (e) and (f) Bistable vibrator, the terminal position is set as the center position, $b_t = 0$. (g) and (h) Asymmetric bistable vibrator, the terminal position is less than the critical position, $b_t < b_c$.

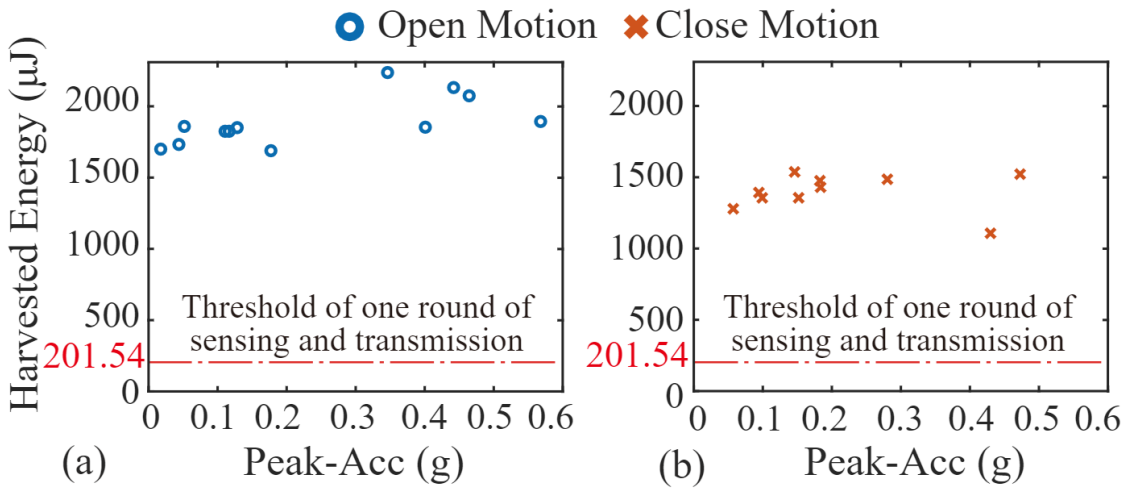

Fig. 6. The harvested energy under various peak accelerations. (a) Open-door motion. (b) Close-door motion.

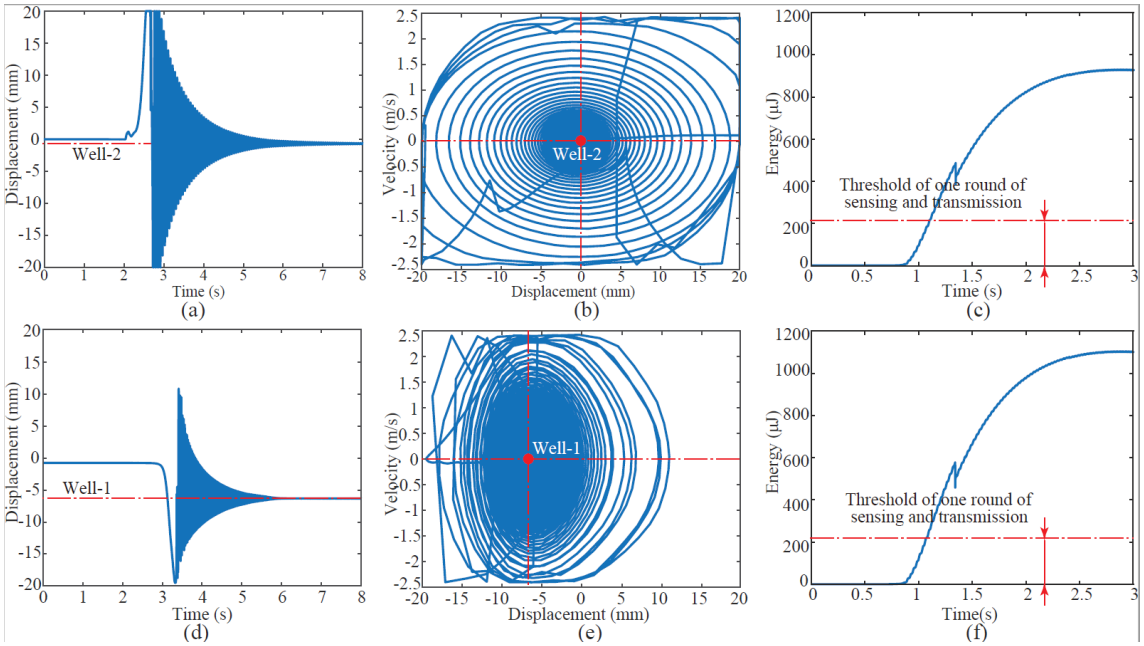

Fig. 7. Experimental results. (a)-(c) Open-door characteristics. (d)-(f) Close-door characteristics. (a) and (d) Beam displacements. (b) and (e) Displacement-velocity phase portraits. (c) and (f) Charging history.

Table 1 Parameters for the transient plucking energy harvester.

Symbol	Description	Value
M	Mass of cantilevered beam with tip magnet	11.7 g
D	Damping coefficient	0.0246 Ns/m
K	Bending stiffness	173.6968 N/m
C_p	Piezoelectric clamped capacitance	37.8412 nF
R	Load resistance	$1.7 * 10^5\ \Omega$
Ψ_e	Electromechanical coefficient	0.13901 mN/V
L	Length of cantilevered beam	105 mm
d_0	Initial vertical interval of the tip magnet and driving magnet	30 mm
V_{O_1}	Volume of tip magnet (M1)	$10 * 10 * 10mm^3$
V_{O_2}	Volume of driving magnet (M2)	$20 * 20 * 20mm^3$
B_r	Residual flux density of magnets	1.2 T
μ_0	Magnetic constant	$4\pi * 10^{-7}$ H/m

References

1. Geoff V. Merrett, B.M.A.-H. *Energy-Driven Computing Rethinking the Design of Energy Harvesting Systems*. in *Design, Automation & Test in Europe Conference & Exhibition (DATE), 2017*. 2017.
2. Liu, H., et al., *A comprehensive review on piezoelectric energy harvesting technology: Materials, mechanisms, and applications.* Applied Physics Reviews, 2018. **5**(4).
3. Fu, H., et al., *Ultra-low frequency energy harvesting using bi-stability and rotary-translational motion in a magnet-tethered oscillator.* Nonlinear Dynamics, 2020. **101**(4): p. 2131-2143.
4. Lan, C., et al., *Magnetically coupled dual-beam energy harvester: Benefit and trade-off.* Journal of Intelligent Material Systems and Structures, 2017. **29**(6): p. 1216-1235.
5. Liang, J., H. Shu-Hung Chung, and W.-H. Liao, *Dielectric loss against piezoelectric power harvesting.* Smart Materials and Structures, 2014. **23**(9).
6. Brandon Lucia, et al. *Intermittent Computing: Challenges and Opportunities*. 2017.
7. Hester, J. and J. Sorber, *The Future of Sensing is Batteryless, Intermittent, and Awesome*, in *Proceedings of the 15th ACM Conference on Embedded Network Sensor Systems*. 2017. p. 1-6.
8. Junrui Liang, X.L., Hailiang Yang, *Kinetic Energy Harvesting Toward Battery-Free IoT: Fundamentals, Co-Design Necessity and Prospects.* ZTE COMMUNICATIONS, 2021. **19**(1).
9. Hester, J. and J. Sorber, *Batteries not included.* XRDS: Crossroads, The ACM Magazine for Students, 2019. **26**(1): p. 23-27.
10. Maria Gorlatova, J.S., Guy Grebla, Mina Cong, Ioannis Kymissis, Gil Zussman, *Movers and shakers: Kinetic energy harvesting for the internet of things.* IEEE Journal on Selected Areas in Communications, 2015. **33(8)**: p. 1624-1639.
11. Fang, S., et al., *A music-box-like extended rotational plucking energy harvester with multiple piezoelectric cantilevers.* Applied Physics Letters, 2019. **114**(23).
12. Fu, X. and W.-H. Liao, *Modeling and Analysis of Piezoelectric Energy Harvesting With Dynamic Plucking Mechanism.* Journal of Vibration and Acoustics, 2019. **141**(3).
13. Fu, H., S. Zhou, and E.M. Yeatman, *Exploring coupled electromechanical nonlinearities for broadband energy harvesting from low-frequency rotational sources.* Smart Materials and Structures, 2019. **28**(7).
14. Li, X., et al., *ViPSN: A Vibration-Powered IoT Platform.* IEEE Internet of Things Journal, 2021. **8**(3): p. 1728-1739.